Supporting information for

A General Approach to Ultrathin NiM (M = Fe, Co, Mn) Hydroxide Nanosheets as High-Performance Low-Cost Electrocatalysts for Overall Water Splitting

Xiuhui Sun,[a] Qi Shao,[a] Yecan Pi,[a] Jun Guo,[b] Xiaoqing Huang[a*]

[a]*College of Chemistry, Chemical Engineering and Materials Science, Soochow University, Jiangsu 215123, China.*

[b]*Testing & Analysis Center, Soochow University, Jiangsu 215123, China.*

X. Sun and Q. Shao contribute equally to this work

Email: hxq006@suda.edu.cn

1: Materials and methods

1.1 Chemicals: Nickel (II) acetylacetonate ($Ni(acac)_2$, 97%), iron (II) acetylacetonate ($Fe(acac)_2$, 97%), cobalt (II) acetylacetonate ($Co(acac)_2$, 97%), manganese (II) acetylacetonate ($Mn(acac)_2$, 97%), and Nafion (5%) were all purchased from Sigma-Aldrich. Ethylene glycol ($(CH_2OH)_2$, 99%), n-butylamine ($C_4H_{11}N$, Analytical Pure) were purchased from Sinopharm Chemical Reagent Co. Ltd. (Shanghai, China). The commercial Pt/C (20 wt%, 2-5 nm Pt nanoparticles) was purchased from Johnson Matthey (JM) Corporation. All the chemicals were used as received without further purification. The water (18 MΩ cm^{-1}) used in all experiments was prepared by passing through an ultra-pure purification system.

1.2 Synthesis of NiFe hydroxide nanosheets (HNSs): In a typical synthesis of NiFe HNSs, 25.6 mg $Ni(acac)_2$, 6.4 mg $Fe(acac)_2$ and 0.2 mL n-butylamine solution were mixed together with 10 mL ethylene glycol and 2 mL deionized water under magnetic stirring. After changed into a clear solution, the mixture was transferred to a 25 mL Teflon-lined stainless-steel autoclave. The sealed vessel was heated at 180 ºC for 5 h, before it cooled to room temperature. The resulting products were collected by centrifugation and washed three times with ethanol (1 mL) / acetone (9 mL) mixture. The syntheses of NiCo HNSs and NiMn HNSs were similar to that of NiFe HNSs, except that $Fe(acac)_2$ was replaced by the equal moles of $Co(acac)_2$ and $Mn(acac)_2$.. The synthesis of $Ni(OH)_2$ nanosheets ($Ni(OH)_2$ NSs) was similar to that of NiFe HNSs, except that precursor was only $Ni(acac)_2$.

1.3 Characterization: The morphologies and sizes of the samples were determined by transmission electron microscope (TEM, Hitachi, HT7700) at 120 kV. High-resolution TEM (HRTEM) and high angle annular dark field scanning TEM (HAADF-STEM) were conducted on an FEI Tecnai F20 transmission electron microscope at an acceleration voltage of 200 kV.

Scanning electron microscope energy-dispersive X-ray (SEM-EDX) characterizations were taken with a HITACHI S-4700 cold field emission scanning electron microscope. Powder X-ray diffraction (PXRD) patterns were collected using an X`Pert-Pro X-ray powder diffractometer equipped with a Cu radiation source (λ = 1.540598 Å). The concentrations of all the catalysts were determined by the inductively coupled plasma atomic emission spectroscopy (710-ES, Varian, ICP-AES).

1.4 Electrochemical measurements: Before the electrochemical tests, the NiM HNSs and $Ni(OH)_2$ NSs were mixed with Vulcan XC-72 carbon in 20 mL of ethanol and sonicated for 1 h. All the samples were then collected by centrifugation, washed with ethanol for three times, and dried under ambient condition. The obtained samples were pulverized, and annealed at 250 ºC under air for 1 h. The final catalysts were redispersed in a mixture solvent containing isopropanol and Nafion (5%) (v : v = 1 : 0.005) to form a homogeneous catalyst ink by sonicating for 30 min. The commercial Pt/C link was prepared by sonicating the commercial Pt/C (JM, 20 wt% Pt on Vulcan XC72R carbon) in an aqueous dispersion (0.4 mg_{Pt} mL^{-1}). 15 μL of the dispersion was transferred onto the glassy carbon electrode (GCE).

A three-electrode system controlled by a CHI660E electrochemistry workstation was used to do the electrochemical measurements. The catalyst ink dropped on the GCE was used as the working electrode. The saturated calomel electrode (SCE) was used as the reference electrode, and graphite electrode or a Pt wire was used as the counter electrode. The reference was calibrated against and converted to the reversible hydrogen electrode (RHE). The cell was purged with O_2 for 30 min prior to each set of experiments, and then blanketed with O_2 during the experiment. Linear sweep voltammetry was carried out at 5 mV s^{-1}, iR drop was compensated at 95% through the positive feedback using the CHI660E electrochemistry workstation. Our typical electrochemical cell had a resistance of about 5 Ω in 1 M KOH. The Tafel slopes were derived from the polarization curves obtained at 1 mV s^{-1} and 95% iR compensation. Chronopotentiometry was carried out under the same experimental setup without compensating iR drop. For overall water splitting chronopotentiometry test, NiFe HNSs was first loaded onto carbon fiber paper to assess its durability. All potentials measured were calibrated to the RHE.

1.5 Calculation of ECAS: The calculation of electrochemically active surface area (ECAS) is estimated from the double layer capacitance (C_{dl}) of the different catalysts in 1 M KOH based on the previous published report.[1-3] The charging current (i_c) was measured from the CVs at different scan rates, as shown in **Figure S4c** and **Figure S13**. The relation between i_c, the scan rate (ν) and the C_{dl} was given in equation (1).

$$i_c = \nu C_{dl} \qquad (1)$$

Therefore, the slope of i_c as a function of ν is equal to Cdl (**Figure 4d**). For the calculation of ECAS, the specific capacitance (Cs) value is 0.040 mF cm^{-2} in 1 M KOH. So the ECAS of is calculated according to equation (2).

$$\text{ECSA} = \frac{C_{dl}}{C_s} \qquad (2)$$

2: Supplementary Figures and Tables.

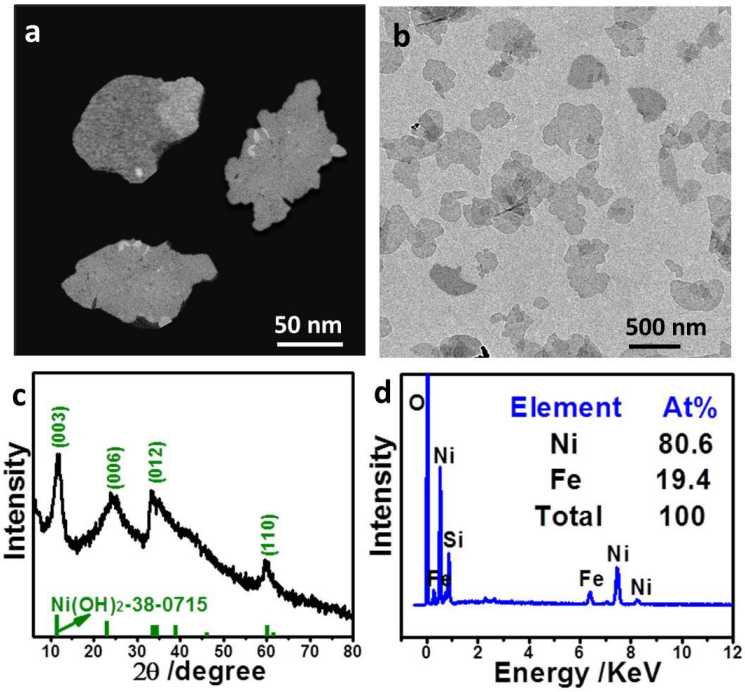

Figure S1. (a) HAADF-STEM image, (b) TEM image, (c) PXRD pattern and (d) SEM-EDX of the NiFe HNSs.

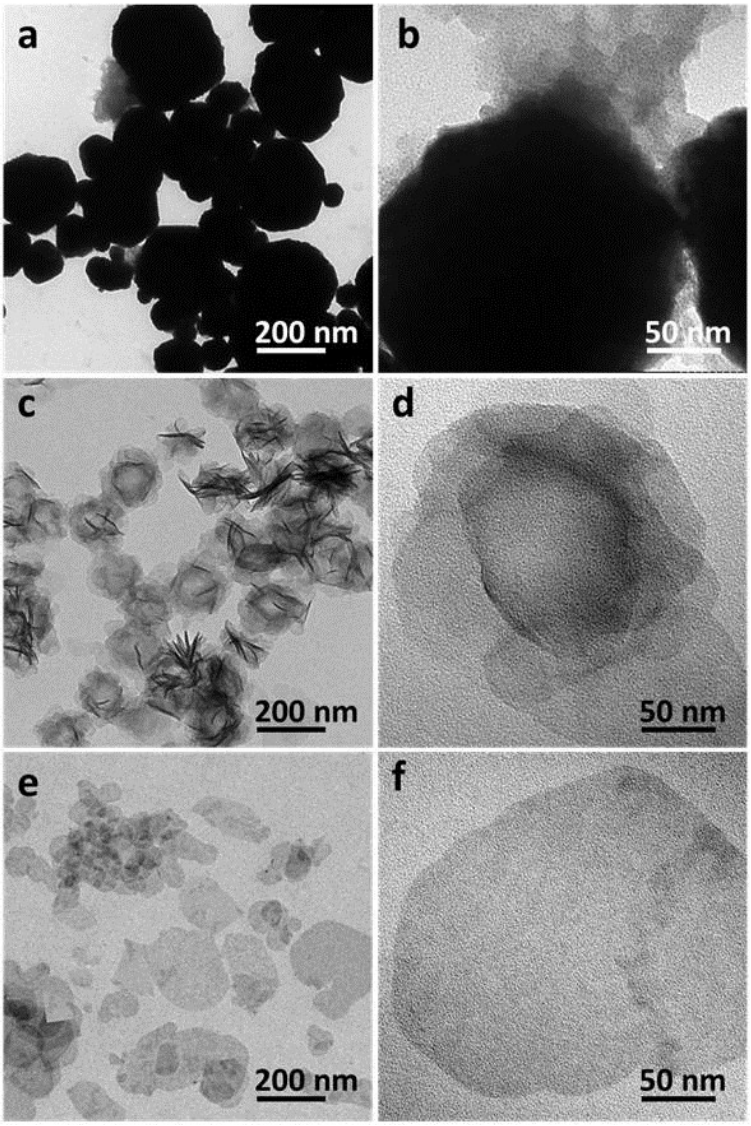

Figure S2. TEM images of the products with the same reaction condition used in the syntheses of NiFe HNSs but (a, b) without using deionized water, (c, d) using 0.5 mL deionized water and (e, f) using 4 mL deionized water.

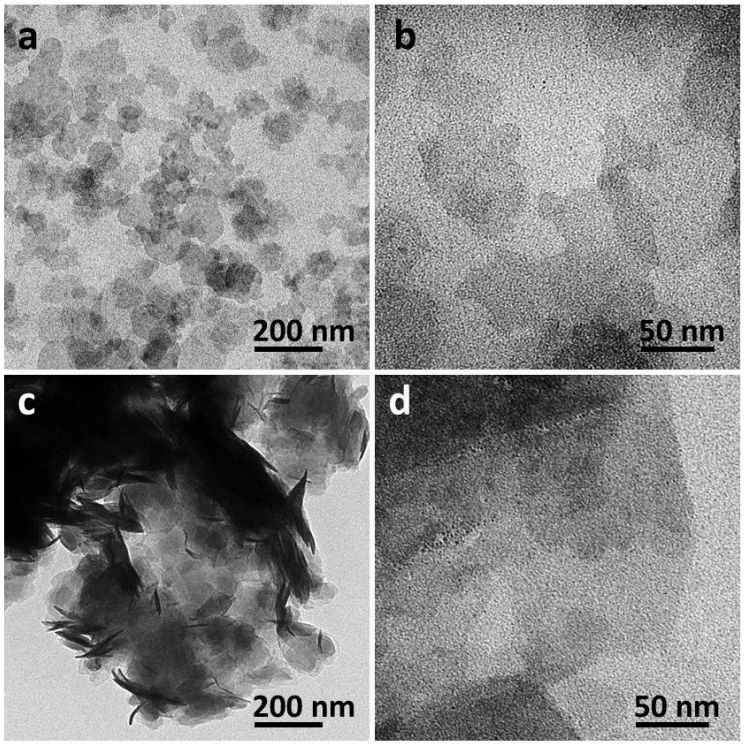

Figure S3. Representative TEM images of the products collected from the reaction with the same condition used in the synthesis of NiFe HNSs but replacing n-butylamine with (a, b) methylamine and (c, d) dodecylamine.

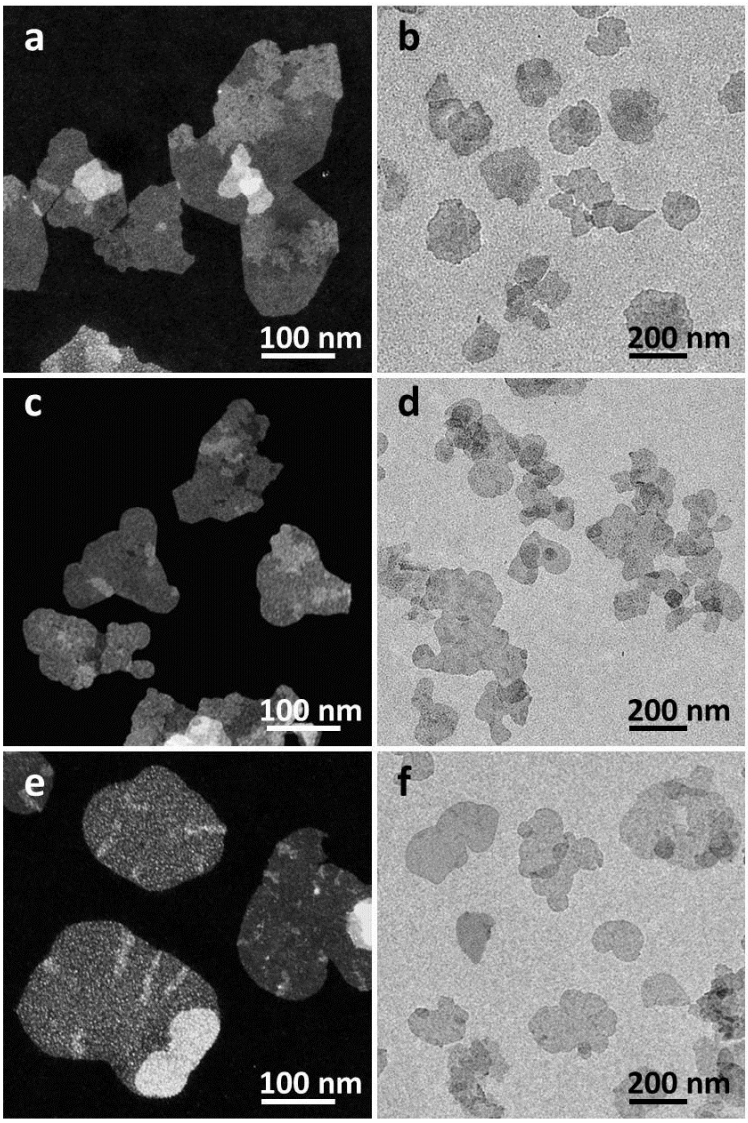

Figure S4. TEM images of (a, b) NiCo HNSs, (c, d) NiMn HNSs and (e, f) $Ni(OH)_2$ NSs.

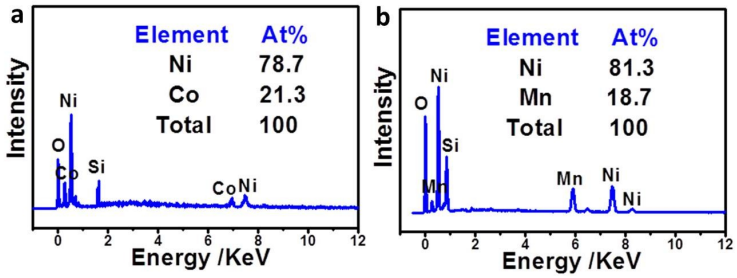

Figure S5. SEM-EDXs of (a) NiCo HNSs and (b) NiMn HNSs.

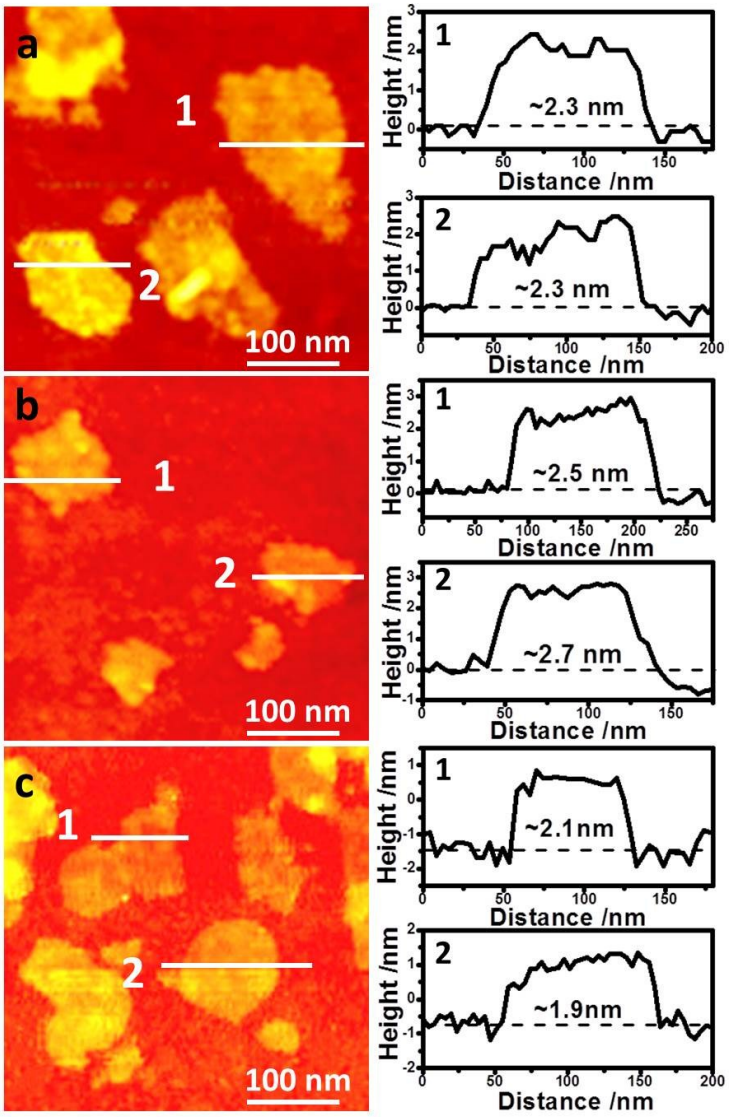

Figure S6. AFM images and corresponding height profiles of (a) NiCo HNSs, (b) NiMn HNSs and (c) $Ni(OH)_2$ NSs.

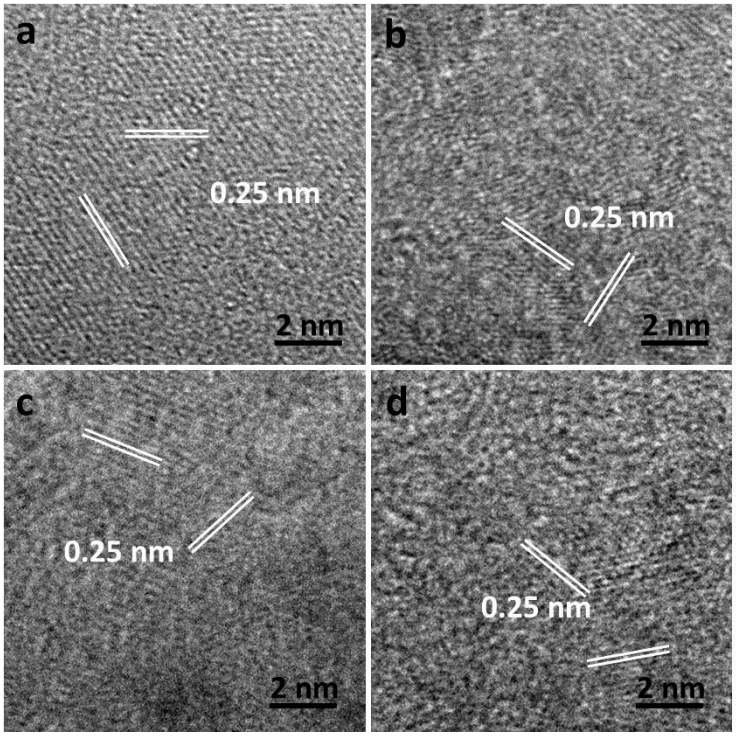

Figure S7. HRTEM images of (a) NiFe HNSs, (b) NiCo HNSs, (c) NiMn HNSs and (d) $Ni(OH)_2$ NSs.

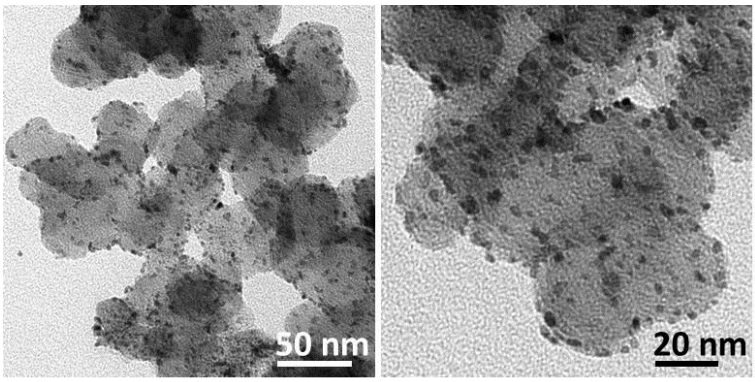

Figure S8. TEM images of the commercial Pt/C.

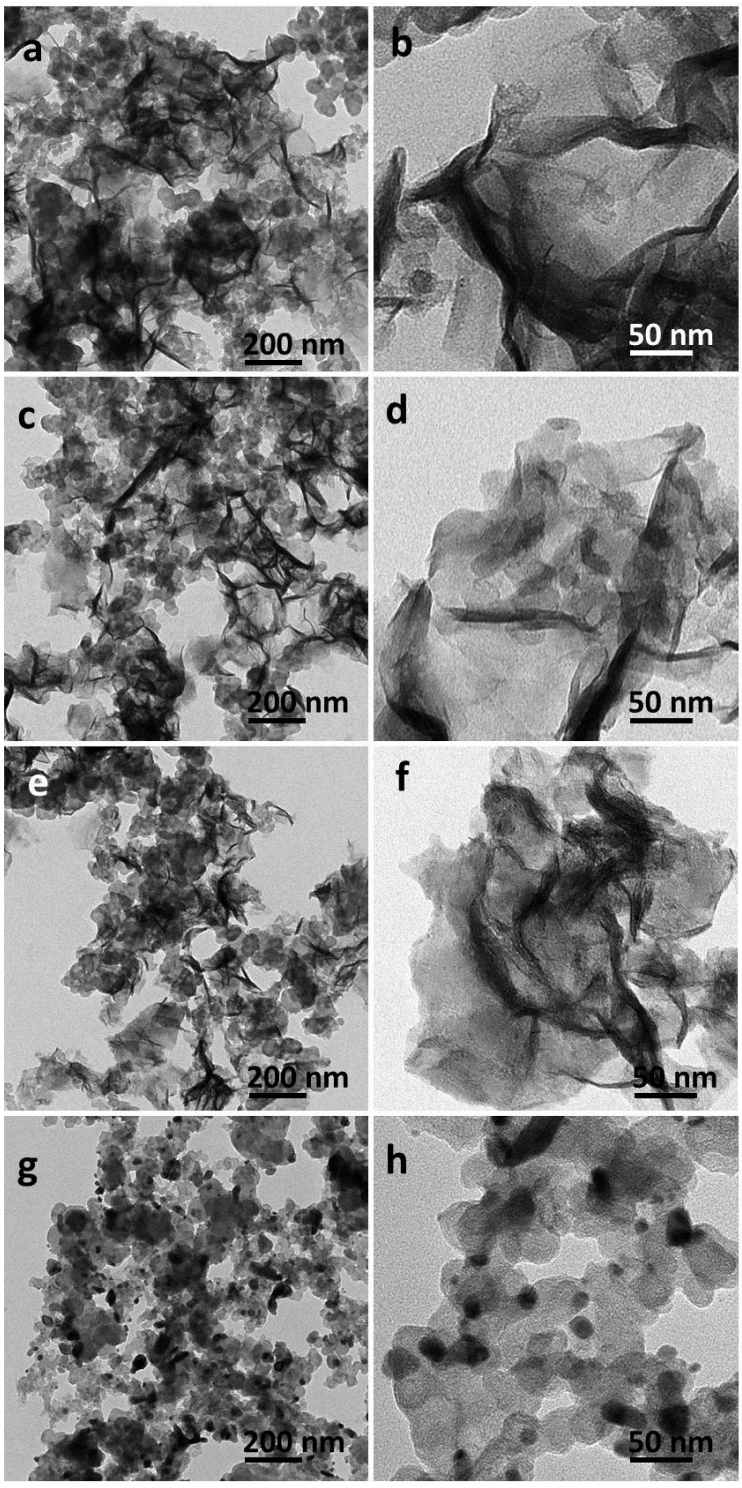

Figure S9. TEM images of NiFe HNSs annealed under air with different temperature treatments: (a, b) 150 ºC, (c, d) 200 ºC, (e, f) 250 ºC and (g, h) 280 ºC for 1h.

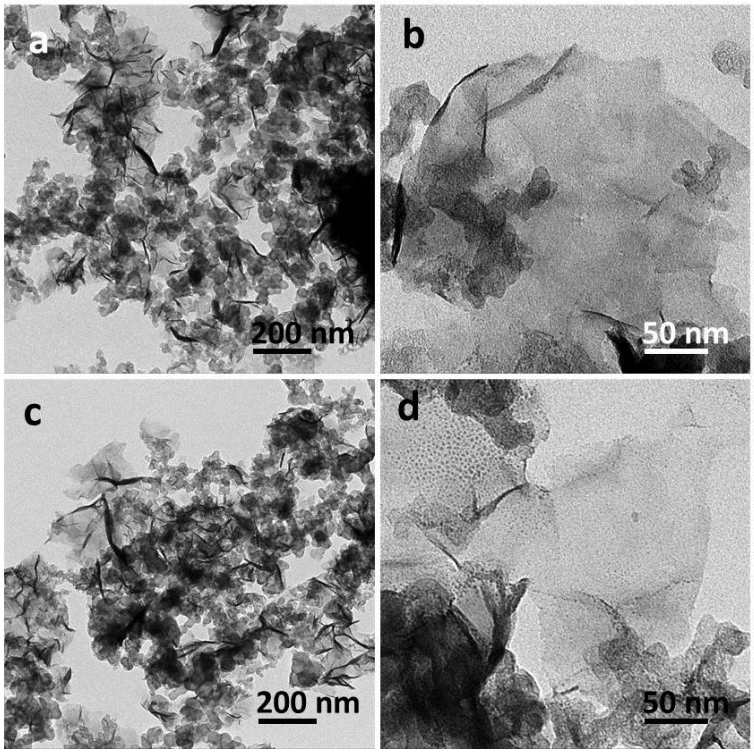

Figure S10. TEM images of NiFe HNSs treated at 250 ºC under air with different time: (a, b) 0.5 h and (c, d) 2 h.

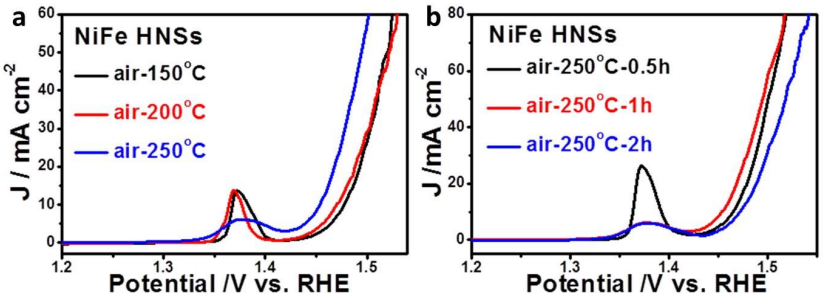

Figure S11. OER polarization curves of NiFe HNSs annealed under air: (a) at different temperature for 1 h and (b) at 250 ºC for different time.

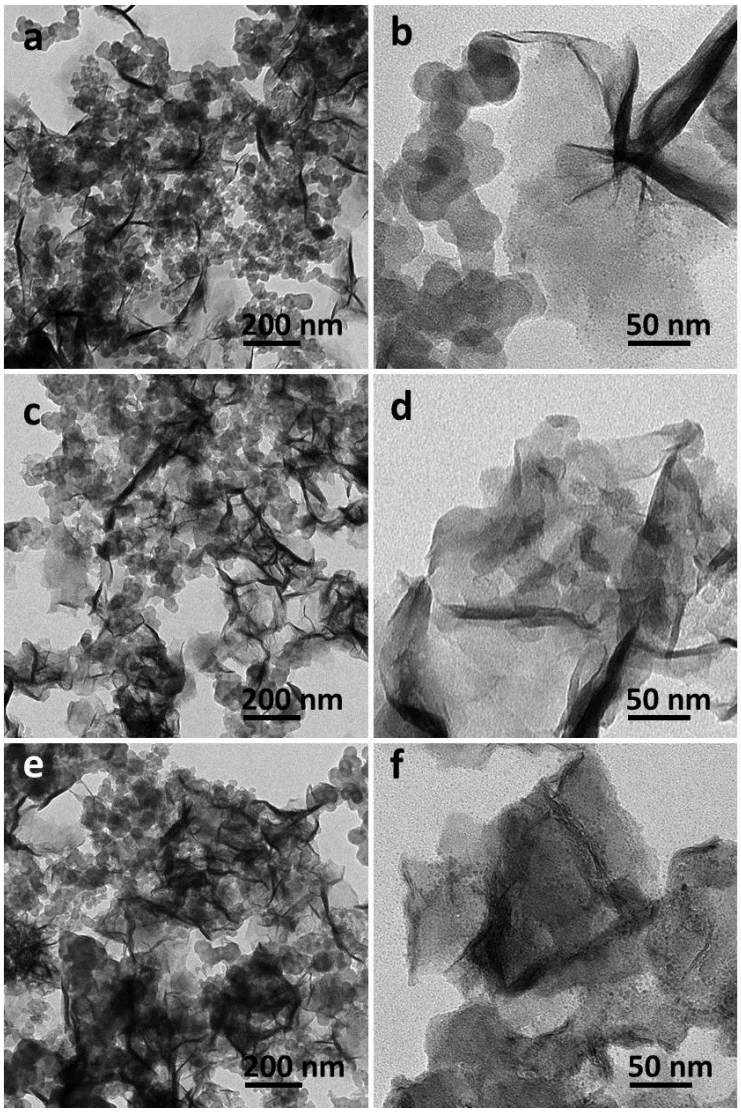

Figure S12. TEM images of (a, b) NiCo HNSs, (c, d) NiMn HNSs and (e, f) $Ni(OH)_2$ NSs annealed at 250 ºC under air for 1h.

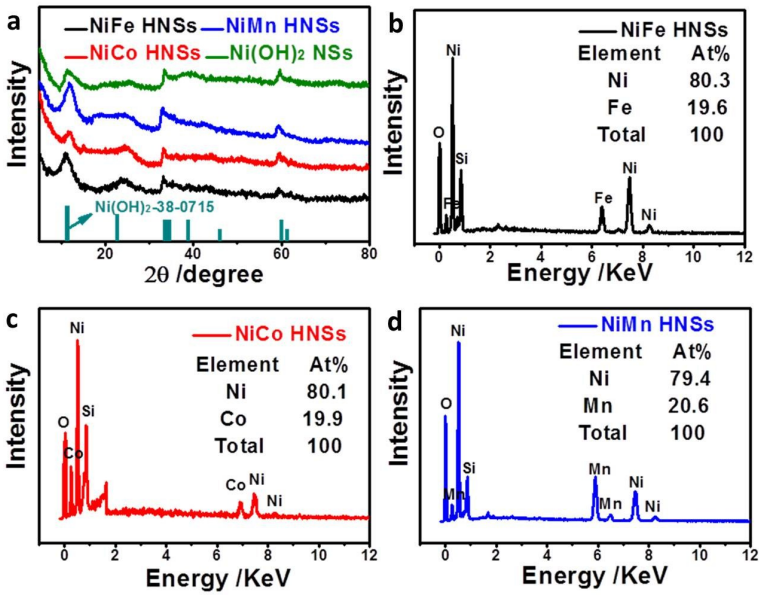

Figure S13. (a) PXRD patternof NiM HNSs and $Ni(OH)_2$ NSs and (b-d) SEM-EDX of the NiFe HNSs, NiCo HNSs, and NiMn HNSs after annealed at 250 ºC under air for 1h.

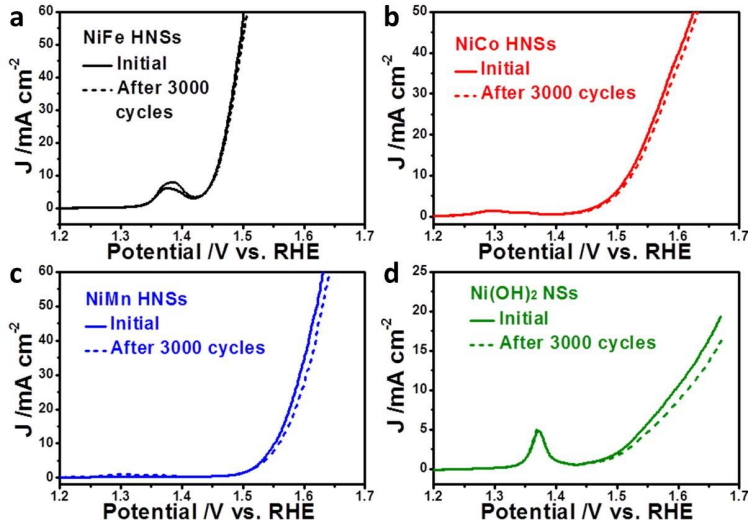

Figure S14. Polarization curves of (a) NiFe HNSs, (b) NiCo HNSs, (c) NiMn HNSs and (d) $Ni(OH)_2$ NSs before and after 3000 CV cycles at scan rate of 50 mV s^{-1}.

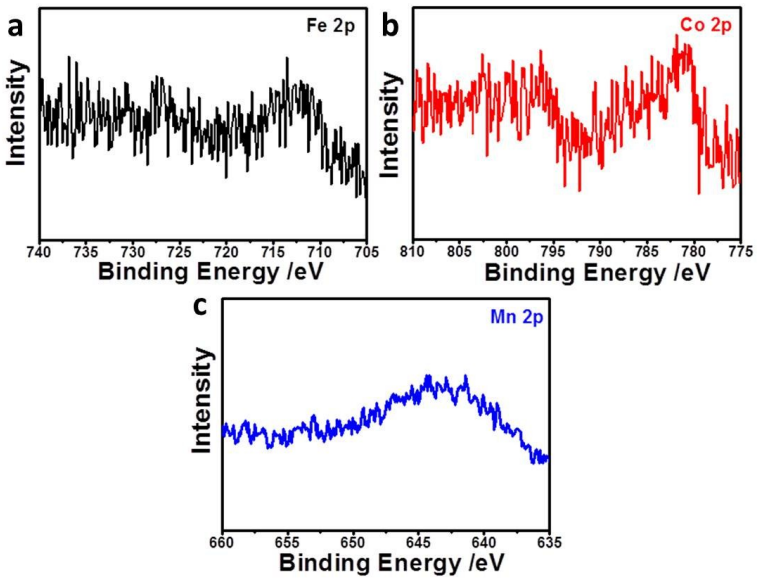

Figure S15. Fe 2p , Co 2p and Mn 2p XPS spectras of NiFe HNSs, NiCo HNSs and NiMn HNSs, respectively.

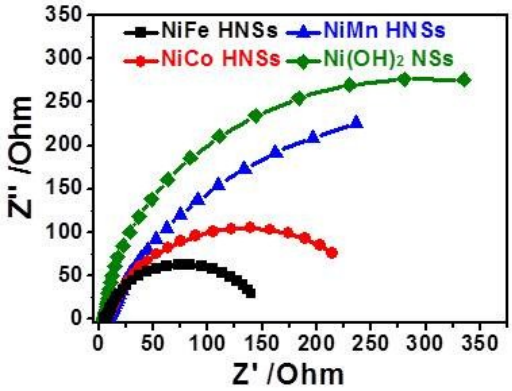

Figure S16. EIS of NiM HNSs and $Ni(OH)_2$ NSs catalyzed OER at overpotential of 300mV over the frequency range 100kHz to 0.1 Hz in 1.0 M KOH.

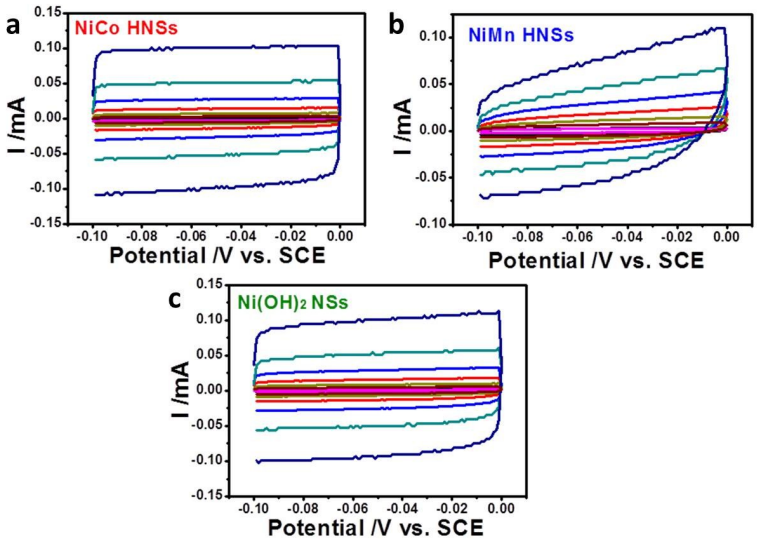

Figure S17. Current measured in the non-faradaic potential from -0.1 V to 0 V at different scan rates of 0.005 (black), 0.01 (red), 0.025 (blue), 0.05 (dark cyan), 0.1 (magenta), 0.2 (dark yellow), 0.4 (navy), and 0.8 V s^{-1} (wine) of (a) NiCo HNSs, (b) NiMn HNSs and (c) $Ni(OH)_2$ NSs.

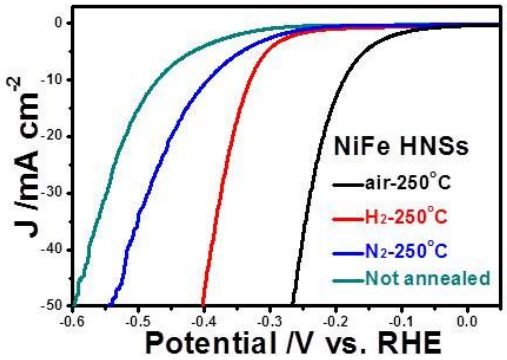

Figure S18. HER polarization curves of NiFe HNSs annealed at different conditions.

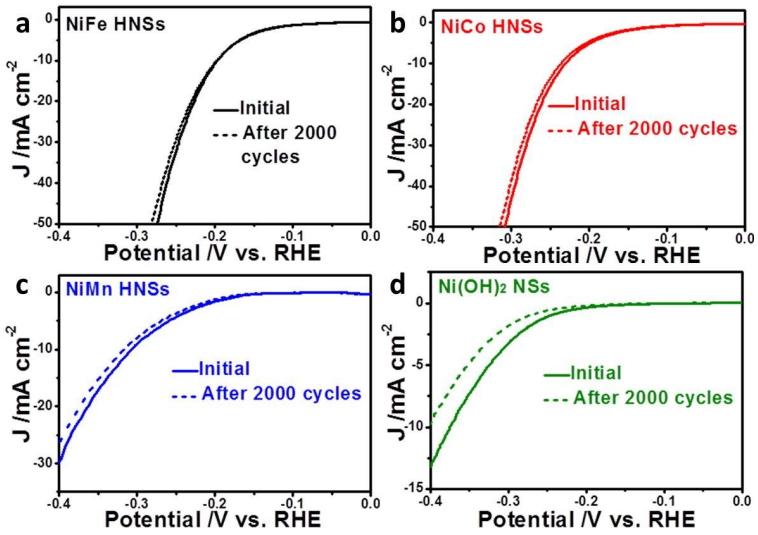

Figure S19. HER polarization curves of (a) NiFe HNSs, (b) NiCo HNSs, (c) NiMn HNSs and (d) $Ni(OH)_2$ NSs before and after 2000 CV cycles at scan rate of 50 mV s^{-1}.

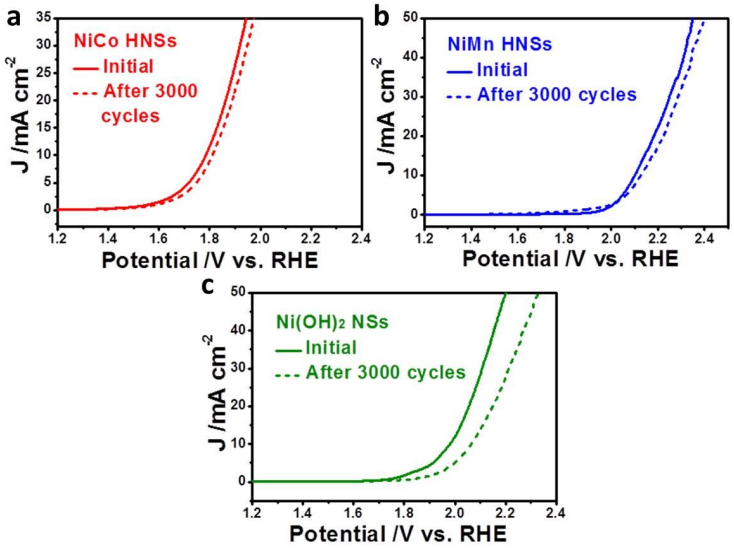

Figure S20. Polarization curves of (a) NiCo HNSs, (b) NiMn HNSs and (c) $Ni(OH)_2$ NSs before and after 3000 CV cycles at scan rate of 50 mV s^{-1}.

Table S1. Comparisons of the catalytic activity of the NiFe HNSs with those of other reported catalysts toward the OER in 1 M KOH.

Catalysts	Overpotentials (mV vs. RHE) at J = 10 mA cm^{-2}	Tafel slopes (mV dec^{-1})	References
NiFe HNSs	220	40.7	**This work**
NiCoP/NF	280	87	*Nano Lett.* **2016**, *16, 7718.*
NiFe/NF	250	57.5	*Nat. Commun.* **2015**, *6*, 6616.
NiSe/NF	270	79	*Angew. Chem. Int. Ed.* **2015**, *54*, 9351.
Ni_5P_4	470	40	*Angew. Chem. Int. Ed.* **2015**, *54*, 12361.
MoO_2/NF	260	54	*Adv. Mater.* **2016**, *28*, 3785.
NiFe LDH/NF	240	/	*Science*, **2014**, *345*, 1593.
CoMn LDH	324	43	*J. Am. Chem. Soc.* **2014***, 136*, 16481.
NiCo LDH/CP	367	40	*Nano Lett.* **2015**, *15*, 1421.
FeCoW	223	37	*Science* **2016**, *352*, 333.
Ni_2P	290	47	*Energy Environ. Sci.* **2015**, *8*, 2347.
Ni_3S_2/NF	260	/	*J. Am. Chem. Soc.* **2015**, 137, 14023.
Cu@CoS*x*/CF	160	/	*Adv. Mater.* **2017**, DOI:10.1002/adma.201606200.

Table S2. Comparisons of the catalytic activity of the NiFe HNSs with those of other reported catalysts toward the HER in 1 M KOH.

Catalysts	Overpotentials (mV vs. RHE) at J = 10 mA cm^{-2}	Tafel slopes (mV dec^{-1})	References
NiFe HNSs	189	78.2	**This work**
Ni_5P_4	150	53	*Angew. Chem. Int. Ed.* **2015**, *54*, 12361.
NiFe LDH/NF	210	/	*Science*, **2014**, *345*, 1593.
Ni_3S_2 Nanosheet Arrays /NF	223	/	*J. Am. Chem. Soc*. **2015**, *137*, 14023.
$CoSe_2$/CC	190	85	*Adv. Mater.* **2016**, *28*, 7527.
CoP/CC	209	129	*J. Am. Chem. Soc.* **2014**, *136*, 7587.
Ni/NiO(OH)/NC	190	44	*Adv. Energy Mater.* **2015**, *5*, 1401660.
Co phosphide/phosphate	380	/	*Adv. Mater.* **2015**, *27*, 3175.
Co, CoOx/CN	232	53	*Angew.Chem. Int. Ed.* **2015**, *127*, 12538.
Ni/NiS	230	123.3	*Adv. Funct. Mater.* **2016**. *26*, 3314.
FeP NAs/CC	220	475	*ACS Catal.* **2014,** *4*, 4065.
Ni_3S_2/NF	223	/	*J. Am. Chem. Soc.* **2015**, 137, 14023.
Cu@CoS*x*/CF	134	61	*Adv. Mater.* **2017**, DOI:10.1002/adma.201606200.

Table S3. Comparisons of the catalytic activity of the NiFe HNSs with those of other reported catalysts toward the overall water splitting in 1 M KOH.

Catalysts	Overall Water Splitting Potentials (V) at J = 10 mA cm^{-2}	References
NiFe HNSs	1.67	**This work**
Ni_5P_4	1.7	*Angew. Chem. Int. Ed.* **2015**, *54*, 12361.
NiFe LDH/NF	1.7	*Science*, **2014**, *345*, 1593.
Ni_3S_2 Nanosheet Arrays /NF	1.76	*J. Am. Chem. Soc*. **2015**, *137*, 14023.
Ni_5P_4 Films/Ni foil	1.7	*J. Am. Chem. Soc.* **2015**, *137*, 2688.
$NiCo_2S_4$/CP	1.68	*Nanoscale* **2015**, *7*, 15122.
Co-P/NC	1.71	*Chem. Mater.* **2015**, *27*, 7636.
Cu@CoS*x*/CF	1.5	*Adv. Mater.* **2017**, DOI:10.1002/adma.201606200.

References:

[S1] C. McCrory, S. Jung, J. Peters, T. Jaramillo, *J. Am. Chem. Soc.* **2013**, 135, 16977-16987.

[S2] X. Lu, C. Zhao, *Nat. Commun.* **2015,** DOI: 10.1038/ncomms7616.

[S3] A. Swesi, J. Masud, M. Nath, *Energy Environ. Sci.* **2016**, 9, 1771-1782.